PHYSICAL REVIEW B VOLUME 27, NUMBER 8 15 APRIL 1983

Site determination for palladium on niobium using angle-resolved photoemission

M. El-Batanouny,* Myron Strongin, and G. P. Williams
Brookhaven National Laboratory, Upton, New York 11973
(Received 8 October 1982)

We demonstrate the possibility of using angle-resolved photoemission from valence levels to gain overlayer site geometry information. To do this we utilize and discuss polarization effects and photoexcitation cross-section effects (as a function of the photon energy). To illustrate the application of the technique we have studied Pd overlayers on Nb(110) and conclude that the Pd(110) overlayer has a hollow-site geometry.

I. INTRODUCTION

In the present paper we demonstrate the possibility of exploiting angle-resolved-photoemission (ARP) techniques to determine the bonding site occupied by an overlayer species. The problem of determining the sites occupied by an atomic or molecular species in an overlayer has been addressed in the past, since such information is an essential ingredient for understanding the properties of these systems. Most of the techniques which have been employed to date are based, one way or another, on the manifestation of multiple-scattering events in the final state of the excited-electron wave function which reflects the geometric environment of the atoms or molecule being studied. Two of these techniques, namely low-energy electron diffraction (LEED) and photoelectron diffraction[1] (PD) involve complex calculation procedures. Furthermore, the former requires long-range order in the overlayers. The latter requires the availability of a suitable core level which, on the one hand, is isolated from other levels so that no distortion of the spectral structures pertaining to that level occurs and, on the other hand, has adequate photoexcitation cross section. Surface extended x-ray-absorption fine structure[2] (SEXAFS) is yet another technique for studying surface geometries which is also based on multiple-scattering effects in the final state. However, the restrictions imposed on the choice of the core level are even more severe in this case than for PD, since the measurements require spectral scans running over several hundreds of volts. These must be free from interferences due to emission from other levels.

The approach we discuss here provides another alternative to the above methods. In contrast to the above techniques it focuses on properties of the initial state which in this case is a valence state of the system that is directly involved in the interaction with the host substrate. To exploit these properties we make use of a combination of two modes of ARP: (1) The photon-energy-dependent (PEARP) mode, and (2) the polarization-dependent (PARP) mode. The latter technique has become an important tool in the study of the electronic structure of solids, surfaces, and chemisorbed layers, while the former has been used mainly to investigate atomic or quasiatomic electronic-related phenomena. The two modes lead to a two-step approach in which we first use the PEARP model to identify the valence states which directly incorporate adatom-substrate interactions and subsequently use the PARP mode to distinguish their symmetry properties. We are then able to derive information about the geometry of the bonding sites.

Gustafsson *et al.*[3] have used a similar technique to determine the orientation of CO on Ni. However, their approach had a different goal and varied conceptually from ours. Their study focused on the angular dependent photoemission from a noninteracting CO orbital. Their conclusions were based on combining these data with previous gas-phase photoelectron spectra and theoretical calculations. No attempts were made to determine the CO bonding site or to investigate the elemental components of the initial state.

II. APPLICATION TO THE Pd-Nb(110) SYSTEM

To illustrate our technique we have chosen to apply it to a particular system which is of current interest to us, namely, a Pd monolayer on the (110) surface of Nb. Recent experiments[4] employing LEED indicated the existence of two structural phases of Pd on the Nb(110) surface. A commensurate (1×1) Pd phase was observed for coverages up to a full monolayer, which we call Pd*(110). Above a monolayer coverage the Pd overlayer was observed to undergo a structural change to an incommensurate phase reminiscent of the fcc(111) surface of pure Pd. Because of large differences in the chem-

isorption activity of the phases these findings spurred considerable interest in the Pd-Nb system, especially towards understanding the electronic properties[5] of the two phases and elucidating the nature of the mechanism involved in the structural phase transition. A knowledge of the sites which the Pd atoms occupy in the Pd*(110) commensurate phase is extremely important in the understanding of these effects and accordingly we choose it as our prototype system.

III. EXPERIMENTAL

All the experiments were done with the use of VG Scientific ADES 400 systems with LEED and Auger-analysis equipment. The synchrotron-radiation work was done at the University of Wisconsin Synchrotron Radiation Center (UWSRC) using a double-grating toroidal monochromator operating at an angle of incidence in zero order of 75°. All the reflections in the beamline are vertical thus maintaining the polarization of the source. The experiments at Brookhaven were done using a conventional (unpolarized) discharge lamp. The Nb substrate used at UWSRC was prepared by recrystallization from a 0.001-in. foil while a Nb single crystal with (110) orientation was used at Brookhaven for part of the polarization-related measurements.

IV. PEAK CHARACTER DETERMINATION

The first step in our approach then deals with using PEARP to sort out from among the spectral peaks those which are involved in the Pd—Nb bonding and which, therefore, incorporate a mixed Pd-Nb character. Such peaks can be associated with initial states which result from Pd-Nb hopping interactions and, therefore, can be expressed as some linear combination of Pd and Nb orbitals. To accomplish this task we have made detailed measurements of the photon-energy dependence of the cross section $\sigma(\hbar\omega)$ of the various ARP peaks which appear in the normal-emission spectra of the Pd-Nb system as well as those of both pure Pd and Nb d states. The purpose of this study was to try to establish a basis for identifying the main components (Pd or Nb $4d$ orbitals or a combination of both) which contribute to a particular peak in the spectrum.

In order to do this it was necessary to study photoemitted peaks over a photon-energy range wide enough to unambiguously reveal atomiclike features in their cross sections as opposed to band-derived features. A second requirement was that there should be no dispersion in the observed peak positions.

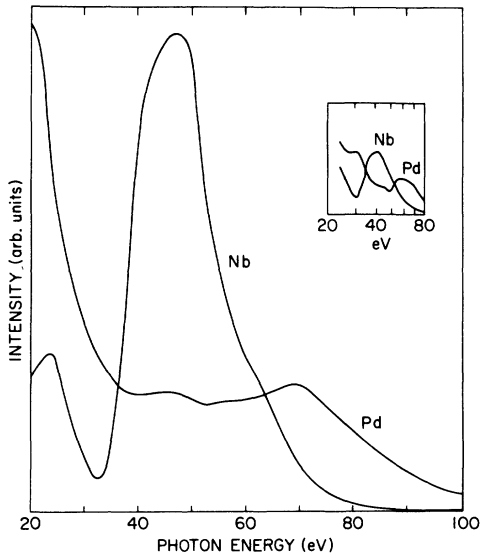

FIG. 1. CIS for pure Nb and pure Pd (normal emission). Both curves have been normalized to the incident-photon flux. Inset shows the photon-absorption spectra of Nb and Pd taken from Ref. 6.

Our measurements spanned the photon energy range from 16—100 eV and were done in the constant initial-energy spectral mode (CIS) where the difference between the analyzer energy and the photon energy is maintained constant, thus directly measuring $\sigma(\hbar\omega)$ for whichever initial energy was chosen. Since these measurements were collected in the normal-emission geometry it was particularly important to establish whether such limited angular-acceptance emission measurements were representative of atomic cross sections. The measured photoexcitation cross sections $\sigma(\hbar\omega)$ of pure Nb and Pd normalized to the photon flux are shown in Fig. 1. In the inset of Fig. 1 we also show the same cross sections as measured by photon absorption.[6]

In Fig. 1, $\sigma^{\mathrm{Nb}}(\hbar\omega)$ exhibits a distinct minimum at about 32 eV almost an order of magnitude below a second maximum at about 45 eV, while $\sigma^{\mathrm{Pd}}(\hbar\omega)$ is almost monotonically decreasing over the range of measurements, with a slight dip at 50—60 eV caused by a Fano resonance and a weak maximum at 70 eV. In addition $\sigma^{\mathrm{Nb}}(\hbar\omega)$ drops more than 2 orders of magnitude from 50—90 eV, while $\sigma^{\mathrm{Pd}}(\hbar\omega)$ falls less than an order of magnitude in the same photon-energy range. The near vanishing of σ^{Nb} at about 90 eV is associated with a Cooper minimum[7] while the strong enhancement in σ^{Nb} between 30 and 50 eV is associated with interferences between $4p$-$4d$ and $4d$-to-ϵf transitions near the Nb $4p$ threshold. Such enhancement has been observed in other transition metals and it is found to decrease in strength with

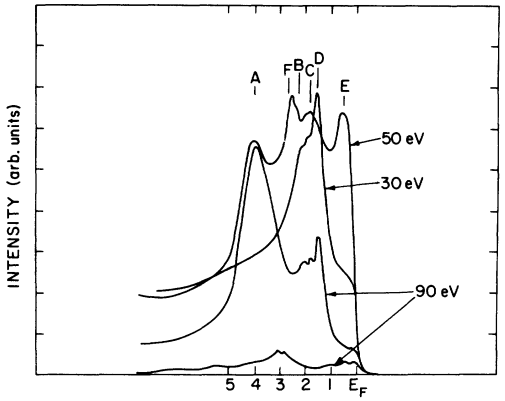

FIG. 2. Normal-emission spectra of Pd*(110) on Nb(110) at different photon energies. (50-eV spectrum is expanded 1.4 times while that at 90 eV is expanded by 3.5 times). Lower-intensity spectrum at 90 eV is for the Nb(110) substrate.

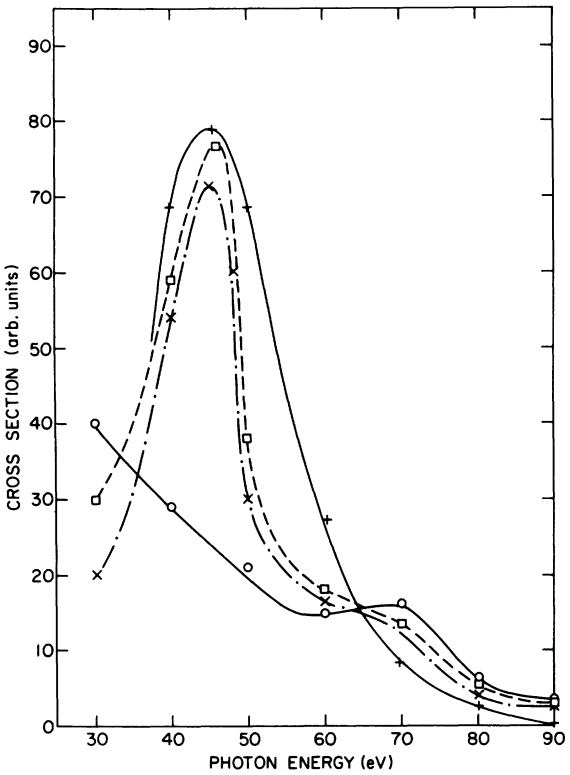

FIG. 3. Photon-energy dependence of peaks *B*, *C*, *D*, and *F* of Fig. 2. □—*B*, ×—*C*, ○—*D*, and +—*F*.

d-band filling. This effect is also confirmed in Fig. 1 when comparing the magnitude of the peak at about 45 eV in σ^{Nb} to that at 70 eV in Pd where the 4*p* threshold is at about 53 and 56 eV.

The data in Fig. 1 thus indicates that broad atomiclike features of the photoexcitation cross sections can indeed be extracted effectively from normal-emission spectra. As we shall demonstrate below, it is by recognizing similar dependencies in cross section from the various valence-band peaks of the combined overlayer-substrate system that we make assignments as to the character of the peaks.

In Fig. 2 we show typical normal-emission spectra of the Pd*(110) phase measured at several photon energies which reflect the trends we discuss below. We have indicated by lines, the locations, and identities of five peaks which we studied. Depending on photon energy and polarization these peaks varied in relative intensity, which is why for a given curve some will appear only as shoulders. The 30-eV photon-energy spectrum is chosen close to the σ^{Nb} minimum (Fig. 1), while the 50-eV spectrum is near the maximum in σ^{Nb} and the 90-eV spectrum near the Nb Cooper minimum. In addition, we have plotted the Nb(110) spectrum measured at 90 eV. Analysis of the 90-eV curves indicates that peaks *A*—*D* incorporate an appreciable Pd *d*-character since, as we have mentioned above and as depicted in the lower 90-eV Nb curve, σ_d^{Nb} almost vanishes at this photon energy, and yet these peaks are quite large by contrast. In Fig. 3 we have plotted the photon-energy dependence of peaks *B*, *C*, *D*, and *F*. A comparison of these curves with σ_d^{Nb} and σ_d^{Pd} of Fig. 1 shows, unambiguously, that peaks *B* and *C* include a Nb *d*-like component, as manifested in the enhancement between 35 and 50 eV, while peak *D* behaves like σ_d^{Pd}. We would like to emphasize at this point that the contributions to peaks *B* and *C* at 90 eV are solely due to the partial Pd *d*-like component in the wave functions of their respective initial states. By contrast, no obvious partial Nb-like wave-function component is observed in peak *D*. Peak *A* also shows very little Nb component in its behavior, and the strong emission of peak *A* at 90 eV compared to other Nb features supports its strong Pd character. Thus, these contrasting behaviors led us to conclude that peaks *B* and *C* are associated with initial states of mixed Pd-Nb *d* character, while peaks *A* and *D* are derived predominantly from Pd *d*-like states. The remaining peaks, i.e., *E* and *F*, which appear at about 0.4 and 2.6 eV below E_F, respectively, are found to be predominantly derived from Nb *d*-like states. Peak *E* has been observed on the clean Nb(110) surface where it appears as the predominant feature in normal emission. Detailed studies of the electronic structure of the Nb(110) surface indicate that this feature persists throughout the surface Brillouin zone[8] (SBZ) and can be attributed to a surface resonance in the vicinity of the SBZ center where it overlaps with an underlaying Σ_1 Nb bulk band. It turns into a pure surface state in

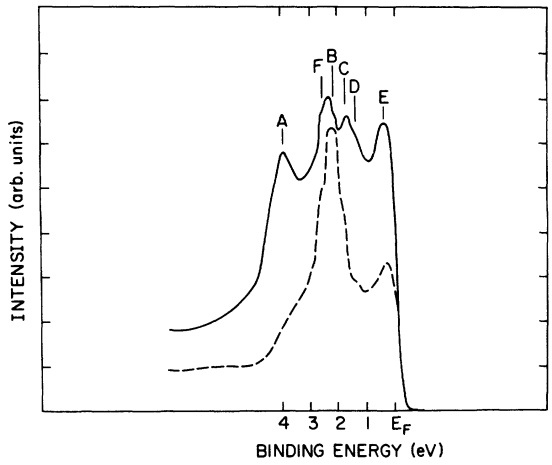

FIG. 4. Photon-polarization dependence of normal-emission spectra of Pd*(110) at $h\nu=50$ eV. Solid curve is for angle of incidence of 45° and dashed curve is 15°.

the outer part of the SBZ where there are no bulk bands with compatible symmetry. The overall dispersion with this peak is about 0.3 eV. Furthermore we found that it tended to broaden and attenuate with surface coverage. All these trends seem to confirm that it is an intrinsic Nb feature and is therefore substrate related and will not be discussed further here. Peak F is best resolved in Fig. 5 where the measurements were made with a He lamp and a lower analyzer pass energy. The photon-energy dependence of peak F is shown in Fig. 3 where the strong similarity with the σ_{Nb} indicates that it is predominantly Nb d-like. This characterization of peak F is further supported by recent calculations of the electronic structure of this system which shows a state of the same symmetry and band ordering and which has a predominant Nb character.

V. PEAK SYMMETRY DETERMINATION

Once the ARP spectral peaks that correspond to the mixed Pd-Nb initial states have been identified, the next step in our scheme is to determine the symmetry character of these states. This is achieved with the use of the PARP mode.

In order for an emitted electron to register at the detector in the angle-resolved mode its wave function should not have a node (i.e., vanish) in the direction of the detector. Since the emitted-electron wave function (EEW) is matched to the surface, it is dressed with the symmetry properties of that surface, i.e., it should belong to some representation of the point-symmetry group of the surface. Thus if the detector is placed in some high-symmetry plane (mirror plane) or along a high-symmetry direction, the absence of a node for an EEW imposes the restriction that the EEW should be invariant with respect to all the symmetry operations that leave the position of the detector unchanged, i.e., with respect to all the operations associated with that particular high-symmetry plane or direction. Restricting the symmetry of the EEW, in turn, through surface matching, requires the final state involved in the photoexcitation process to have the same symmetry.

A second requirement for detection of an electron is the nonvanishing of the photoexcitation matrix element. This requires that the matrix-element integrand be also an invariant quantity with respect to the point-group operation and leads to rules governing the polarization selectivity. The invariance of both the integrand and the final-state wave function leads to the condition of invariance of the product

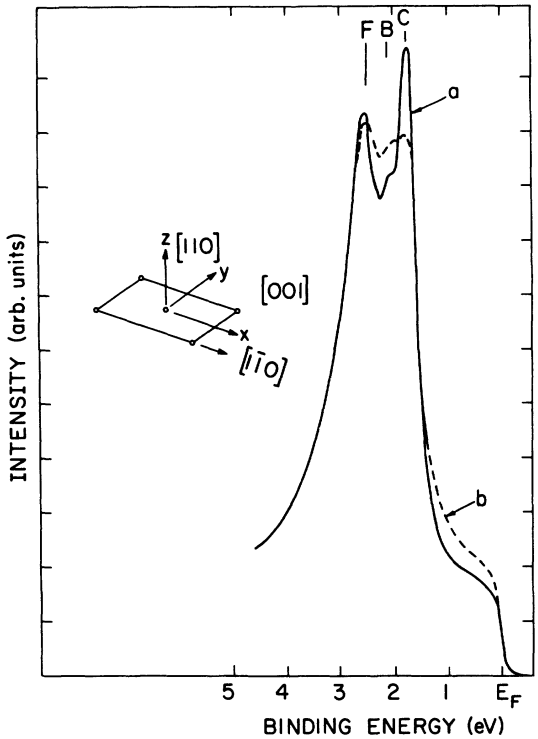

FIG. 5. Photon-polarization dependence in normal emission of peaks B and C ($h\nu=21.2$ eV). In curve a, the plane of incidence is the yz plane, and in curve b, the plane of incidence is the xz plane. Geometry is illustrated in the inset. Curves have been normalized to peak F which because of its $d_{3z^2-r^2}$ or $d_{x^2-y^2}$ symmetry is not expected to depend on the position of the plane of incidence. Note that the angle of incidence of the light (ψ) is slightly different in curves a and b. For curve b, $\psi=60$, and for curve a, $\psi=45°$. Analysis of data on different runs shows that the shapes of the curves are insensitive to ψ over this range. This change in ψ does however lead to the necessity of normalizing to peak F.

of the dipole operator and the initial-state wave function.[9] In other words, one can judiciously select the incident-light-sample—analyzer geometry to exploit effectively the optical dipole-selection rules.

The commensurate Pd monolayer Pd*(110) has the point-group symmetry of the (110) surface of bcc Nb, namely C_{2V}. This twofold symmetry comprises a twofold rotation about the surface normal (the z axis is chosen normal to the surface plane along the bulk [110] direction, while the x and y axes are chosen along the [1$\bar{1}$0] and [001] directions, respectively; see inset of Fig. 5), and two reflection planes, namely xz and yz planes. These operations render states of $d_{3z^2-r^2}$ and $d_{x^2-y^2}$ character invariant, and they consequently can be photoexcited to invariant final states (which are detectable in normal emission) only via the invariant component of the field, which is that component normal to the surface $A_\perp$. States with d_{xz} and d_{yz} character are invariant only with respect to reflection through the xz and yz planes, respectively, and, therefore, are connected to invariant final states via the x and y components of the field, respectively $A_{||}^{x,y}$. Finally, states with d_{xy} character cannot be photoexcited to invariant final states, and hence cannot be detected in normal emission. This prescription thus provides a viable scheme for determining the orbital character of the initial states of interest.

The variation of the magnitudes of the $A_\perp$ and $A_{||}$ polarization components was accomplished by changing the angle of incidence of light. Figure 4 shows normal-emission spectra for Pd*(110) measured at 50-eV photon energies at two angles of incidence: 45° where the $A_\perp$ component has an appreciable amplitude and 15° where the $A_\perp$ almost vanishes. We observe that peaks A, D, and F show strong dependence on $A_\perp$; as a matter of fact, they are dramatically attenuated at 15° angle of incidence. This behavior led us to conclude that these peaks are associated with initial states of $d_{3z^2-r^2}$, $d_{x^2-y^2}$, or s character, or a mixture of such orbitals.

The remaining peaks (B and C) show contrasting behavior from peaks A, D, and F in their polarization dependence. They are effectively increased in amplitude as $A_\perp$ is decreased and $A_{||}$ increased. This becomes evident after a decomposition of the peaks seen in curves a and b of Fig. 5. This implies that these peaks correspond to d_{xz}- and d_{yz}-like initial states.

Furthermore, to differentiate between d_{xz}- and d_{yz}-like states we use the fact that orbitals of d_{xz} symmetry can be photoexcited to a detectable final state only via the x component of the $A_{||}$, while d_{yz} is excited via the y component. Unfortunately since unpolarized (He I) light had to be employed in this experiment, it was impossible to completely eliminate one of these polarization components. However, by calculating[10] the angle-of-incidence dependence of the amplitudes of the individual polarization components we found the result that around 45°—60° angles of incidence the ratio of $P_{||}/P_\perp \approx 0.7$ where $P_{||}$ and $P_\perp$ are the components of $A_{||}$ parallel to and perpendicular to the plane of incidence, respectively. Notice that the photon energy used is above the bulk-plasma frequencies of both Nb and Pd and therefore above any characteristic ω_p of the overall system.

Rotating the sample by 90° about the surface normal allows us to interchange the directions of $P_{||}$ and $P_\perp$ with respect to the x and y directions and, in turn, with respect to d_{xz}- and d_{yz}-like states. Figure 5 shows the results of these measurements where the two curves were normalized to peak F which, as discussed above, is of $d_{3z^2-r^2}$ or $d_{x^2-y^2}$ symmetry and is not affected by the rotation.

We can see that the intensities of peaks B and C do change as the directions are interchanges: peak C decreases relative to B as the [1$\bar{1}$0] direction is changed from $P_\perp$ to along $P_{||}$. The data also suggest, as expected, that C decreases absolutely as the [1$\bar{1}$0] direction changes from $P_\perp$ to $P_{||}$, while B increases through this rotation. Note that the assignment of C or B to d_{xz} or d_{yz} is not totally conclusive because of the small effect with unpolarized light. The use of polarized light would clear up this difficulty. We emphasize, however, that the present data do conclusively demonstrate that the bonding-orbital symmetry is d_{xz} or d_{yz} and therefore, as will be seen, allow determination of the site geometry.

VI. DISCUSSION AND CONCLUSIONS

We have characterized the compositions and symmetries of the initial states that contribute to the measured ARP spectra and have investigated and selected from among these states the ones that incorporate the Pd-Nb character. Our subsequent task, then, is to investigate the compatibilities of these states with those expected from the various possible bonding site geometries on the Nb(110) surface. The relatively close metallic radii of Nb and Pd constrain the possible bonding sites to three models involving top, hollow, or bridge sites.

In the top-site geometry it is expected—according to a simple tight-binding approach—that the $d^{\mathrm{Pd}}_{3z^2-r^2}$-$d^{\mathrm{Nb}}_{3z^2-r^2}(dd\sigma)$ interactions would be either dominant or at least equal to the d^{Pd}_{xzyz}-$d^{\mathrm{Nb}}_{xzyz}(dd\pi)$ interactions. This translates to having $d_{3z^2-r^2}$-like states with Pd-Nb mixing equal to or even stronger than that in d_{xz}- or d_{yz}-like states. Relating this to

our data, we find that the $d_{3z^2-r^2}$ orbitals observed are almost decoupled: The 4-eV state is predominantly Pd d-like and the 2.6-eV state is predominantly Nb. We conclude therefore that the top-site geometry is very unlikely.

Similar arguments can be employed to examine the candidacy of the two remaining sites. In both the bridge-site geometry and the hollow-site geometry there are two first- and two second-nearest-neighbor Nb atoms. However, if we assume a first-nearest-neighbor distance (d_1) equal to the average d_1 of pure Nb and pure Pd (d_1 of Nb and Pd differ by about 3%) we find that $d_2/d_1 \approx 0.9$ for the hollow site and ≈ 0.7 for the bridge site. Since the hopping interaction[11] τ scales approximately as $(1/d)^5$ we find that in the hollow-site geometry $\tau_2/\tau_1 \approx 0.6$ while in the bridge-site geometry $\tau_2/\tau_1 \approx 0.14$. Subscripts 1 and 2 refer to the first- and second-nearest neighbor, respectively. Thus the hopping interaction between the Nb substrate and the Pd overlayer would be much stronger for the hollow than for the bridge site. For the hollow site then it would not be surprising to find considerable Nb contributions to both the d_{xz} and d_{yz} bonding states. This is indeed observed in Fig. 3 in the cross-section dependence and in Fig. 2 in the energy-distribution curves. Comparing curves at 30 and 90 eV we would estimate a Nb contribution to peaks B and C of around 50%.

We have applied the combined techniques of PARP and PEARP to the problem of overlayer geometry. To do this we have discussed the various selection rules and photoexcitation cross sections and illustrated their application with the use of spectra taken for the Pd-Nb(110) system. We have attempted to show the strengths as well as weaknesses in these techniques. Thus although the site geometry is not yet firmly established by the technique there are other advantages in applying them to other systems, the most important ones being the lack of need for long-range order or a suitable core level. As the technique is applied further (initially to well known systems) and as experience of using it is gained it will become more powerful for determining structures. Indeed one can already use the technique to establish whether low-coverage overlayer geometries resemble those at higher coverages where LEED or other information is available.

ACKNOWLEDGMENTS

We have profited from discussions with J. Davenport, W. Eberhardt, D. Hamann, and S. L. Weng. We acknowledge considerable collaboration from Ed Rowe and colleagues at UWSRC and E. Jensen, T. Rhodin, and R. Merrill of Cornell University. Work performed at Brookhaven National Laboratory is supported by the Division of Materials Sciences, U.S. Department of Energy, under Contract No. DE-ACO2-76CHO0016. The Synchrotron Radiation Center at the University of Wisconsin—Madison is supported by the National Science Foundation (NSF) under Grant No. DMR-77-21888 and the Cornell facility by NSF Grant No. DMR-77-05078-A2.

---

*Now at Physics Department, Boston University, Boston, Massachusetts 02215.

[1]D. P. Woodruff, D. Norman, B. W. Holland, N. V. Smith, H. H. Farrell, and M. M. Traum, Phys. Rev. Lett. 41, 1130 (1978).

[2]E. A. Stern, Phys. Rev. B 10, 3027 (1974); see also a review article in Rev. Mod. Phys. 53, 769 (1981).

[3]T. Gustafsson, E. W. Plummer, D. E. Eastman, and J. L. Freeouf, Solid State Commun. 17, 391 (1977).

[4]M. Strongin, M. El-Batanouny, and M. A. Pick, Phys. Rev. B 22, 3126 (1980).

[5]M. El-Batanouny, M. Strongin, G. P. Willliams, and J. Colbert, Phys. Rev. Lett. 46, 269 (1981).

[6]J. H. Weaver and C. G. Olsen, Phys. Rev. B 14, 3251 (1976).

[7]U. Fano and J. W. Cooper, Rev. Mod. Phys. 40, 441 (1968).

[8]M. El-Batanouny, unpublished results.

[9]J. Hermanson, Solid State Commun. 22, 9 (1977).

[10]This calculation was made using the ϵ values from J. H. Weaver, D. W. Lynch, and C. G. Olsen, Phys. Rev. B 7, 4311 (1973).

[11]W. A. Harrison and S. Froyen, Phys. Rev. B 21, 3214 (1981).